Available online at www.sciencedirect.com
ScienceDirect
Journal of Power Sources 177 (2008) 24–32
JOURNAL OF POWER SOURCES
www.elsevier.com/locate/jpowsour

Nickel catalysts supported on ZrO_2, Y_2O_3-stabilized ZrO_2 and CaO-stabilized ZrO_2 for the steam reforming of ethanol: Effect of the support and nickel load

J.D.A. Bellido, E.M. Assaf *

Instituto de Química de São Carlos, Universidade de São Paulo, Av. Trabalhador Sãocarlense 400, 13566-590 São Carlos, SP, Brazil

Received 25 September 2007; received in revised form 24 October 2007; accepted 4 November 2007
Available online 12 November 2007

Abstract

Catalysts with various nickel loads were prepared on supports of ZrO_2, ZrO_2–Y_2O_3 and ZrO_2–CaO, characterized by XRD and TPR and tested for activity in ethanol steam reforming. XRD of the supports identified the monoclinic crystalline phase in the ZrO_2 and cubic phases in the ZrO_2–Y_2O_3 and ZrO_2–CaO supports. In the catalysts, the nickel impregnated on the supports was identified as the NiO phase. In the TPR analysis, peaks were observed showing the NiO phase having different interactions with the supports. In the catalytic tests, practically all the catalysts achieved 100% ethanol conversion, H_2 yield was near 70% and the gaseous concentrations of the other co-products varied in accordance with the equilibrium among them, affected principally by the supports. It was observed that when the ZrO_2 was modified with Y_2O_3 and CaO, there were big changes in the CO and CO_2 concentrations, which were attributed to the rise in the number of oxygen vacancies, permitting high-oxygen mobility and affecting the gaseous equilibrium. The liquid products analysis showed a low selectivity to liquid co-products during the reforming reactions.

Keywords: Nickel catalyst; ZrO_2; Y_2O_3-stabilized ZrO_2; CaO-stabilized ZrO_2; Ethanol steam reforming

1. Introduction

Ethanol steam reforming has been investigated in recent years as a renewable resource that could supply part of the world energy demand, with low environmental impact and a high proportion of hydrogen among the products. This reaction offers an alternative to methane-reforming (non-renewable) reactions. The development of ways to produce hydrogen by ethanol steam reforming has been studied over the last decade by many researchers [1–6]. Among the various advantages of using ethanol as reagent in steam reforming are renewable fuel, high-hydrogen content, low toxicity, safe storage, transport and handling [7–9].

The reactions involved in ethanol steam reforming are thermodynamically favorable at temperatures above 573 K, hydrogen, carbon oxides and methane being the main gaseous products. [4]. A number of catalytic systems have been tested for this reaction, from those involving noble metals [10–12] to transition metals such as cobalt and nickel [1,9,13–15].

Nickel catalysts supported on ZrO_2 supports have been tested for methane-reforming reactions [16–18]. The ZrO_2 exhibits thermal stability, electrical conductivity and oxygen vacancies, and its properties can be improved by the introduction of lanthanide and alkaline-earth cations such as Y^{3+}, La^{3+}, Ca^{2+} or Mg^{2+} into the ZrO_2 lattice [19,20]. The replacement of the Zr^{4+} cation with one of these cations with lower positive charge leads to a negative overall charge that is compensated by an increased number of oxygen vacancies, to maintain electrical neutrality. Consequently, the oxygen ionic mobility is enhanced. These modifications in the ZrO_2 support can activate the gaseous oxygen-producing O^{2-} or O^- species which facilitates hydrocarbon oxidation [5].

The objective of this work was to study the role of supports ZrO_2 and ZrO_2 modified with CaO and Y_2O_3 on the performance of nickel catalysts in the steam reforming of ethanol,

* Corresponding author. Tel.: +55 1633739951; fax: +55 1633739952.
E-mail address: eassaf@iqsc.usp.br (E.M. Assaf).

0378-7753/$ – see front matter © 2007 Published by Elsevier B.V.
doi:10.1016/j.jpowsour.2007.11.006

as well as the effect of the nickel load supported on yttrium-stabilized zirconia.

2. Experimental

2.1. Catalyst preparation

Nickel catalysts were prepared on three different commercial supports: zirconia (Aldrich), yttrium-stabilized zirconia (Aldrich) and calcium-stabilized zirconia (Aldrich). An aqueous solution of $Ni(NO_3)_2{\cdot}3H_2O$ was used to impregnate the support at 60 °C for 3 h, which was then dried at 60 °C for 12 h and finally calcined at 700 °C for 2 h in air (30mL min^{-1}). The catalysts were prepared with a nickel load of 5 wt.%. On the yttrium-stabilized zirconia was deposited 5 wt.%, 10 wt.% and 15 wt.% of the nickel.

In this paper, the supports are referred to as Z, YSZ and CSZ for zirconia, yttrium-stabilized zirconia and calcium-stabilized zirconia, respectively. The catalysts with nickel load of 5 wt.% were named as 5NiZ, 5NiYSZ and 5NiCSZ and the catalysts with a nickel load of 5 wt.%, 10 wt.% and 15 wt.%, supported on YSZ are named as 5NiYSZ, 10NiYSZ and 15NiYSZ, respectively.

2.2. Characterization

The crystalline phases were identified in a Carl Zeiss-JENA URD-6 X-ray diffractometer with nickel-filtered Cu Kα radiation (λ = 1.5406 Å, 40 kV, 30 mA), data being collected in the range $2\theta = 3$–$80°$, at a scan speed of $2°\ min^{-1}$.

Temperature-programmed reduction (TPR) was performed in a quartz tube reactor using a Micromeritics Chemisorb 2705 analyzer. Hydrogen consumption was measured by a thermal conductivity detector (TCD). In the analyses, 50 mg sample was placed in the reactor and reduced with a 5%H_2:95%He (v/v) gas mixture. The temperature was increased to 1000 °C at a heating rate of 10 °C min^{-1}. A standard CuO powder was used to calibrate the amount of H_2 consumed.

2.3. Ethanol steam reforming

Catalytic reactions were carried out with 150 mg catalyst in a fixed-bed down-flow quartz reactor (i.d. = 13 mm) connected inline to a gas chromatograph fitted with a TCD. Prior to reactions, the catalysts were activated by reduction with H_2 (30 mL h^{-1}) at 750 °C for 3 h. The reactions were carried out at 500 °C and 600 °C, using an ethanol:water mixture in a molar ratio 1:3, with a feed-rate of 2.5 mL h^{-1}. The reaction temperature was measured and controlled by a thermocouple inserted directly into the top of the bed catalyst.

The gaseous products of reaction were analyzed inline with a gas chromatograph (Varian, Model 3800) with two thermal conductivity detectors and an automated injection valve. The reaction outlet stream was divided into two aliquots in which different products were analyzed, in order to measure all the reaction products accurately. One of the aliquots was used to analyze hydrogen and methane, which were separated in a 13× molecular sieve-packed column, using nitrogen as carrier gas. The other aliquot, carried in a stream of He, was used to analyze CO, CO_2, CH_4, and C_2H_4, which were separated in 13× molecular sieve and porapak-N-packed columns.

After the reactions, some catalysts were submitted the elemental analysis for carbon determination using an Elemental Analyzer CE1110, model CHNS-0, with 3 mg of the sample in a tin capsule, and the furnace at 1200 °C.

3. Results and discussion

3.1. Catalysts with 5 wt.% Ni supported over Z, YSZ and CSZ

3.1.1. Characterization of catalysts

The XRD spectra of the supports Z (ZrO_2), YSZ (ZrO_2 stabilized with Y_2O_3) and CSZ (ZrO_2 stabilized with CaO) are shown in Fig. 1. The spectrum for support Z shows the main peaks characteristic of the monoclinic phase, at 2θ: 28°, 31.5°, 49.3° and 50.3°; and this is the stable phase at room temperature. The YSZ and the CSZ supports show the main peaks at 2θ: 29.8°, 34.8°, 50.1° and 59.6°, characteristic of the cubic phase according to the JCPDS pattern: 77-2119 and 23-0341 for YSZ and CSZ, respectively [21]. The higher crystallinity of the commercial supports indicates a very low supported surface area.

The XRD spectra of the catalysts with 5 wt.% nickel are shown in Fig. 2. Each catalyst shows, besides the respective support peaks reported in Fig. 1, two peaks at 2θ: 37.3° and 43.3°, which are characteristic of the NiO crystalline phase (JCPDS 44-1159), and no other nickel phase was observed.

The TPR profiles of the 5NiZ, 5NiYSZ and 5NiCSZ catalysts are shown in Fig. 3. None of the supports showed any reduction peaks, owing to their high thermal stability [22]. The profiles

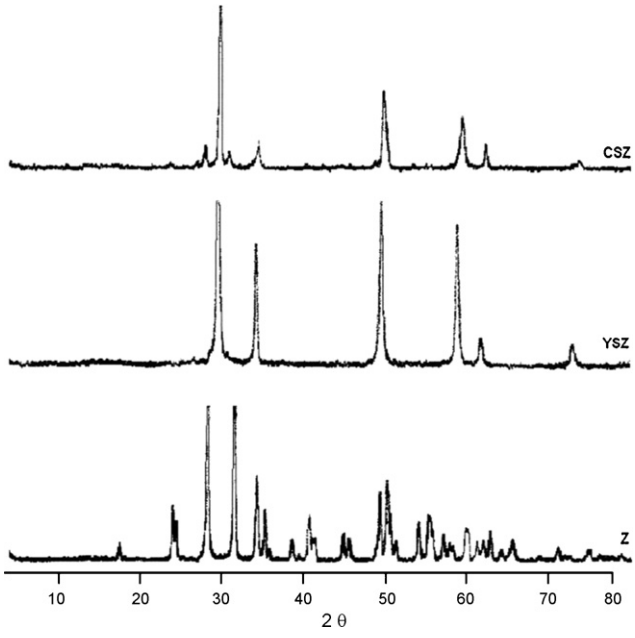

Fig. 1. X-ray diffraction patterns of Z, YSZ and CSZ supports.

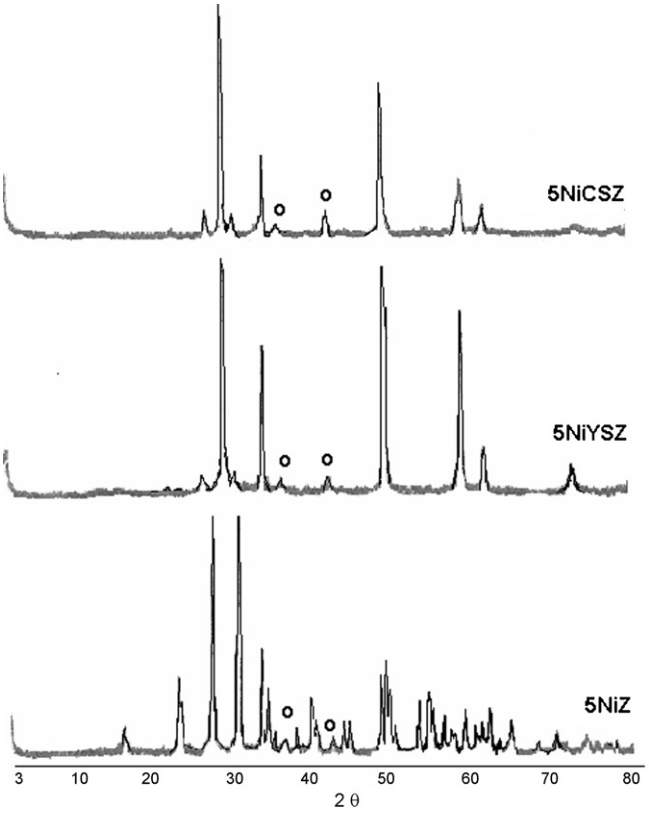

Fig. 2. X-ray diffraction patterns of 5NiZ, 5NiYSZ and 5NiZ catalysts, NiO (◯).

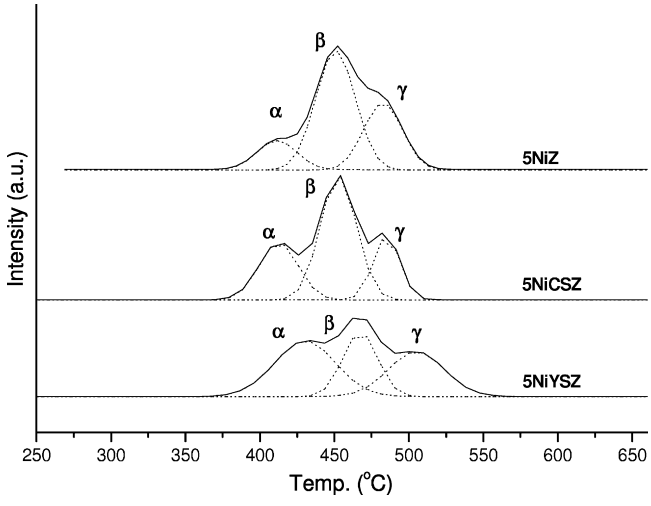

Fig. 3. TPR patterns of nickel catalysts: 5NiZ, 5NiYSZ and 5NiCSZ.

Table 2
Mean composition of the gaseous products (%) of ethanol steam reforming

Temperature (°C)	Catalyst	Gaseous products (%)			
		H_2	CH_4	CO	CO_2
500	5NiZ	50	21	23	6
	5NiYSZ	56	18	12	12
	5NiCSZ	55	15	15	10
600	5NiZ	57	10	19	15
	5NiYSZ	67	6	12	15
	5NiCSZ	68	7	13	12

for the nickel catalysts exhibit more than one reduction peak, indicating reducible nickel species that interact differently with the support.

Table 1 shows the integrated values of H_2 consumed in the TPR peaks of the catalysts. All peaks were attributed to the reduction of Ni^{2+} species to Ni^0 directly without going through other nickel species. Some authors attribute the peak at the lowest temperature like nickel species in the form of crystallites and the peaks at higher temperatures are nickel species in close contact with the supports [23,24]. However, as was mentioned previously, among the principal characteristics of the zirconia supports is the presence of oxygen vacancies and the effect of the interaction between these oxygen vacancies and the oxides impregnated on the zirconia on their redox behavior has been reported by many authors working with different metal oxide systems that use zirconia-based oxides as supports [25,26]. Thus the reduction peak at low temperature has been attributed to the reduction of NiO influenced by the oxygen vacancies. These oxygen vacancies facilitate the reduction of these NiO species by weakening the Ni–O bond or polarizing the H_2 molecule, which is more reactive for the reduction of NiO in the vicinity of the oxygen vacancies. The detection of NiO reflections in the XRD spectra of the catalysts (Fig. 2) indicates the presence of crystallites of NiO. These NiO crystallites give rise to the second reduction peak. The third reduction peak can be attributed to the reduction of NiO species that interact strongly with the supports, but are not in contact with the oxygen vacancies.

3.1.2. Catalytic tests of the samples with 5 wt.% Ni supported on Z, YSZ and CSZ

Figs. 4 and 5 show the product composition profile during the reaction time. All the catalysts were stable throughout the period of reaction (6 h). The mean composition of the gaseous products is reported in Table 2.

The ethanol conversions achieved by the catalysts are presented in Table 3, together with the main liquid products

Table 1
H_2 consumed in the reduction of nickel catalysts, 5NiZ, 5NiYSZ and 5NiCSZ

Catalyst	H_2 consumed $\times 10^{+5}$ (TPR peak temperature (°C))			Total H_2 consumed $\times 10^{+5}$
	α	β	γ	
5NiZ	0.6 (410)	2.4 (450)	1.4 (483)	4.4
5NiCSZ	1.2 (410)	2.4 (450)	0.9 (483)	4.5
5NiYSZ	1.7 (430)	1.1 (462)	1.3 (504)	4.1

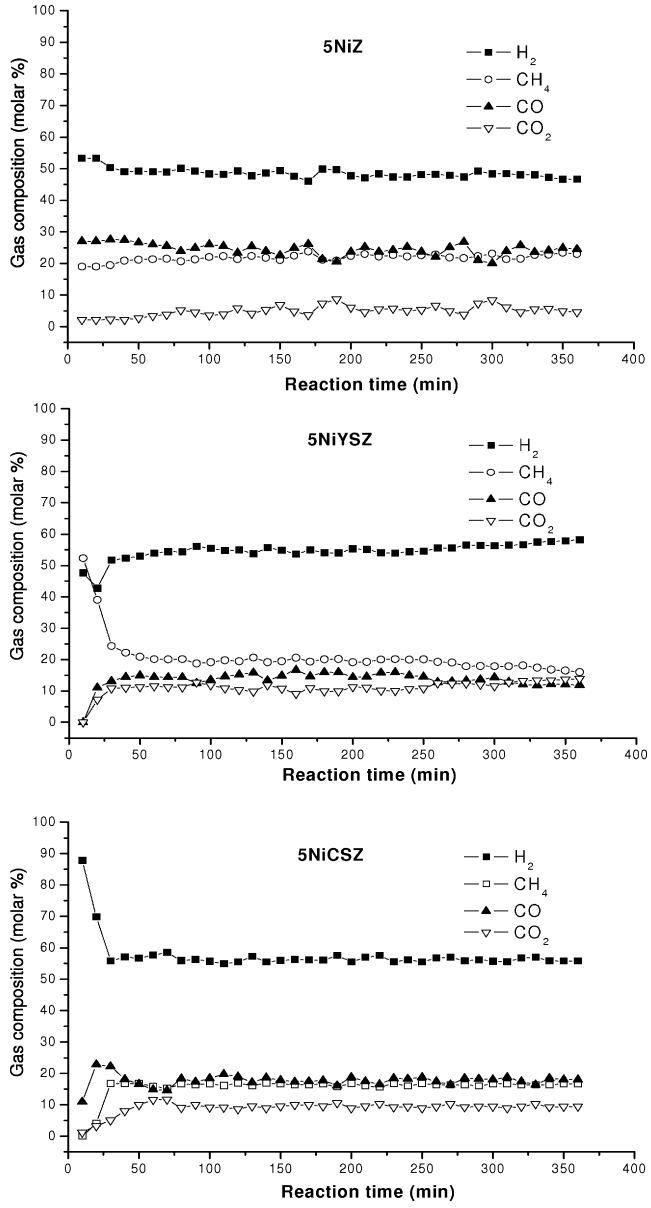

Fig. 4. Gas composition of the ethanol steam reforming products as a function of reaction time. Reaction temperature 500 °C.

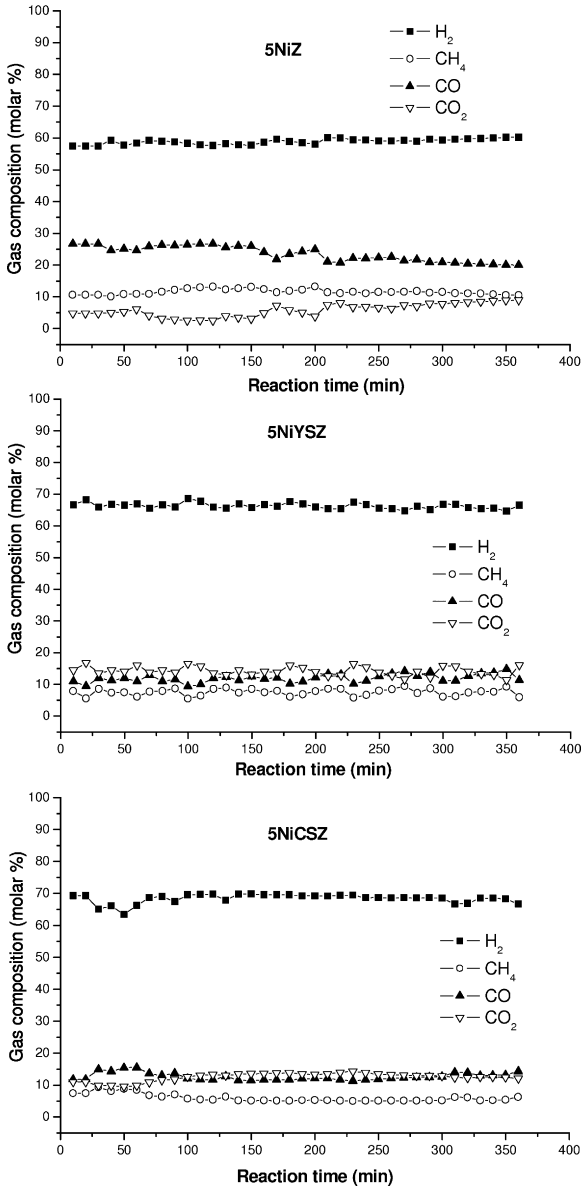

Fig. 5. Gas composition of the ethanol steam reforming products as a function of reaction time. Reaction temperature 600 °C.

collected after 6 h of reaction. Ethyl ether, acetone, ethyl acetate and acetic acid were observed in trace amounts.

The gaseous products obtained suggest that nickel-based catalysts supported on ZrO_2 and modified ZrO_2 show C–C bond-braking activity. The main products are H_2, CH_4, CO and CO_2. Ethylene (C_2H_4) is present in negligible levels due to the weakly acid character of the support, this being the condition necessary for the dehydration reaction to occur.

Table 3
Ethanol conversion and composition of liquid effluents after 6 h of reaction

Temperature (°C)	Catalyst	Volume of liquid effluents (mL)		Water consumption (%)	Ethanol conversion (%)
		Acetaldehyde	Ethanol		
500	5NiZ	0.0	0.0	8	99.5
	5NiYSZ	0.2	0.7	3	90.7
	5NiCSZ	0.1	1.4	–	82.5
600	5NiZ	0.0	0.1	8	99.2
	5NiYSZ	0.0	0.1	28	98.6
	5NiCSZ	2.0	3.3	–	58.2

From a thermodynamic view, the steam reforming of ethanol is energetically favorable; however, the reactions involving water and ethanol can follow various pathways, depending on the operation conditions, such as, pressure, temperature and water/ethanol molar ratio.

Among the several reactions that could occur [27], and taking into account the experimental results obtained here, those that best represent the ethanol steam reforming are

$$C_2H_5OH + 3H_2O \rightarrow 6H_2 + 2CO_2 \quad (1)$$

$$C_2H_5OH \rightarrow CH_3CHO + H_2 \quad (2)$$

$$CH_3CHO \rightarrow CH_4 + CO \quad (3)$$

$$C_2H_5OH \rightarrow H_2 + CO + CH_4 \quad (4)$$

$$C_2H_5OH + H_2O \rightarrow 4H_2 + 2CO \quad (5)$$

$$C_2H_5OH + H_2O \rightarrow 2H_2 + CO_2 + CH_4 \quad (6)$$

$$CH_4 + 2H_2O \rightarrow 4H_2 + CO_2 \quad (7)$$

$$CO + H_2O \rightarrow H_2 + CO_2 \quad (8)$$

$$CH_4 \rightarrow 2H_2 + C \quad (9)$$

$$2CO \rightarrow CO_2 + C \quad (10)$$

Considering reaction (1), with the molar ratio H_2O:C_2H_5OH of 3:1, the steam reforming of ethanol could reach a maximum production of 75%H_2 and 25%CO_2, however, the presence of CH_4 and CO in the products indicates that other parallel reactions are occurring.

The reactions (2) and (3) are summed in reaction (4). This pathway is suggested by the acetaldehyde observed, in this study, in the liquid by-products. The decomposition reaction (4) gives an equimolar fraction (33.3%) of all three gaseous products, H_2, CO and CH_4.

The proportion of H_2 in the products is higher for the 5NiYSZ and 5NiCSZ catalysts (56% and 55%, respectively) than for the catalyst 5NiZ (50%) at 500 °C (Fig. 4 and Table 2), and these values are accompanied by a diminution in the CH_4 concentration for the 5NiYSZ and 5NiCSZ catalysts (18% and 15%, respectively), compared to the 5NiZ catalyst (21%). This behavior suggests that CH_4 decomposition (reaction (9)) may occur more readily over the 5NiYSZ and 5NiCSZ catalysts. The high CO_2 concentration produced on the 5NiYSZ and 5NiCSZ catalysts (12% and 10%, respectively), compared to the 5NiZ catalyst (6%), could indicate promotion of the Boudard reaction (reaction (10)), whereas the greater consumption of water observed with the 5NiZ catalyst suggests that the water–gas shift reaction (reaction (8)) may be favored by the unmodified zirconia.

Reactions (5) and (6), being thermodynamically spontaneous, are theoretically possible pathways, but the high concentration of hydrogen in reaction (5) and of CO_2 in reaction (6) argue against this possibility. Conversely, the presence of acetaldehyde among the liquid by-products suggests that the decomposition of ethanol to acetaldehyde, follow the reaction (2), and subsequently the decomposition of acetaldehyde by reaction (3), are the steps coherent with the results obtained in this work.

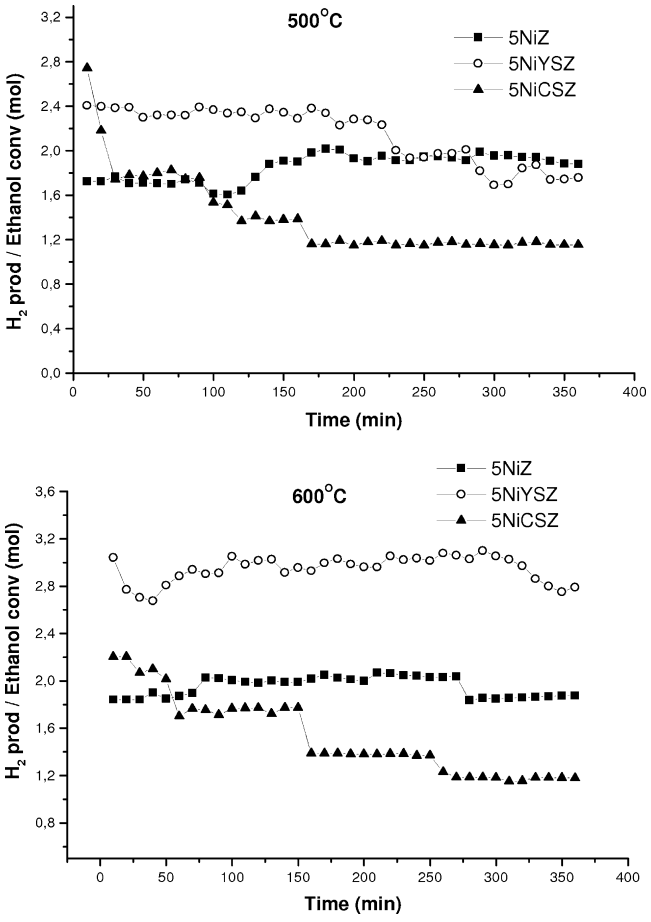

Fig. 6. Hydrogen selectivity in the ethanol steam reforming at 500 °C and 600 °C.

When the temperature of the catalytic tests was increased to 600 °C, higher proportion of H_2 and CO_2 were produced on the 5NiYSZ and 5NiCSZ catalysts than on the 5NiZ catalyst, and less CH_4, indicating that the steam reforming of CH_4 (reaction (7)) could be favored at the higher temperature, especially on the 5NiYSZ catalyst. This hypothesis is supported by the large water consumption on this catalyst. The lower H_2 production and CH_4 consumption on 5NiZ suggest that on this catalyst the water–gas shift reaction might prevail over the steam reforming of CH_4.

Fig. 6 shows the hydrogen selectivity results at 500 °C and 600 °C. It is observed that the 5NiCSZ catalyst showed the worst performance at both temperatures, with the ethanol conversion being smaller at 600 °C and producing acetaldehyde, explaining its poor hydrogen selectivity, as can be seen in Table 3. It can also be seen that, although at 500 °C the levels of hydrogen production on the 5NiZ and 5NiYSZ catalysts are practically the same, at 600 °C the hydrogen selectivity of the 5NiYSZ catalyst is appreciably higher than that of the 5NiZ catalyst.

Many authors [28,29] have reported the participation of zirconia and modified zirconias not only as supports, but also participating actively in the catalytic process, especially in reactions such as CH_4 reforming and CO oxidation. Jackson and

Ekerdt [30] have reported that the active sites for CO reaction on ZrO_2, or ZrO_2 doped with Y_2O_3, are their anionic oxygen vacancies and that the reaction velocity is controlled by the mobility of anions through the oxygen vacancies. The purpose of modifying the zirconia with Y_2O_3 and CaO is to enhance its conductive properties by increasing the quantity of oxygen vacancies. As can be observed, the distribution of the gaseous products changes markedly when the pure ZrO_2 support is modified. The CO concentration shows a strong decrease when the support used is modified zirconia. This behavior may be attributed a more activation of the compound contained oxygen, due to the increase in surface oxygen vacancies on the modified zirconia (CSZ and YSZ) that could favor a rise in the proportion of CO_2.

On the other hand, with respect to the hydrogen production (Fig. 6) the addition of Ca^{2+} and Y^{3+} cations to the ZrO_2 lattice causes different changes in behavior relative to pure ZrO_2, pure when the reaction temperature is increased from 500 °C to 600 °C. As can be seen, the use of the ZrO_2 modified with Y^{3+} (YSZ) leads to an improvement in the selectivity to hydrogen compared to the pure ZrO_2 support, while this does not occurs when the support used is ZrO_2 modified with Ca^{2+} (CSZ), which presents the same performance that of pure ZrO_2. These results suggest that the increase in oxygen vacancies in the support does not, by itself, lead to improvement of the catalytic performance; other interactions between the impregnated nickel species and the supports should be important for catalytic behavior. Wang et al. [31] studied the dry reforming of methane on a nickel catalyst supported on ceria doped with yttrium, where they suggest that the improvement of the catalytic performance is due to a synergic effect between the nickel species and oxygen vacancies, forming active centers of Ni-Ce^{3+} at the interface. Considering these results, the interactions of the nickel species that favored the catalytic performance could depend on the cation added. In the present case, the interactions between nickel and the surface oxygen vacancies on the support with formation of a Ni-Y^{3+} couple, provide a better catalytic response than with the couple Ni-Ca^{2+}. Further studies may help us to understand how these interactions occur.

The elemental analysis showed that the catalysts based on modified zirconia support catalysts, 5NiYSZ and 5NiCSZ, after 6 h of reaction at 600 °C presented higher carbon formation rate (0.027 mmol C min^{-1} and 0.021 mmol C min^{-1}, respectively) than the pure-zirconia, 5NiZ (0.010 mmol C min^{-1}). This it could be due to the modified support have presented more activity for the CH_4 decomposition and Boudard reactions (reactions (9) and (10), respectively).

3.2. Effect of the nickel load supported on YSZ

Catalysts were made by supporting various nickel loads (5 wt.%, 10 wt.% and 15 wt.%) on YSZ and the effects of these loads on their characteristics and ethanol steam-reforming activity were observed.

Fig. 7 shows the XRD spectra of these catalysts, where in addition to the XRD peaks assigned to the support and discussed previously, peaks are observed that related to the NiO phase, increasing in intensity with the NiO load.

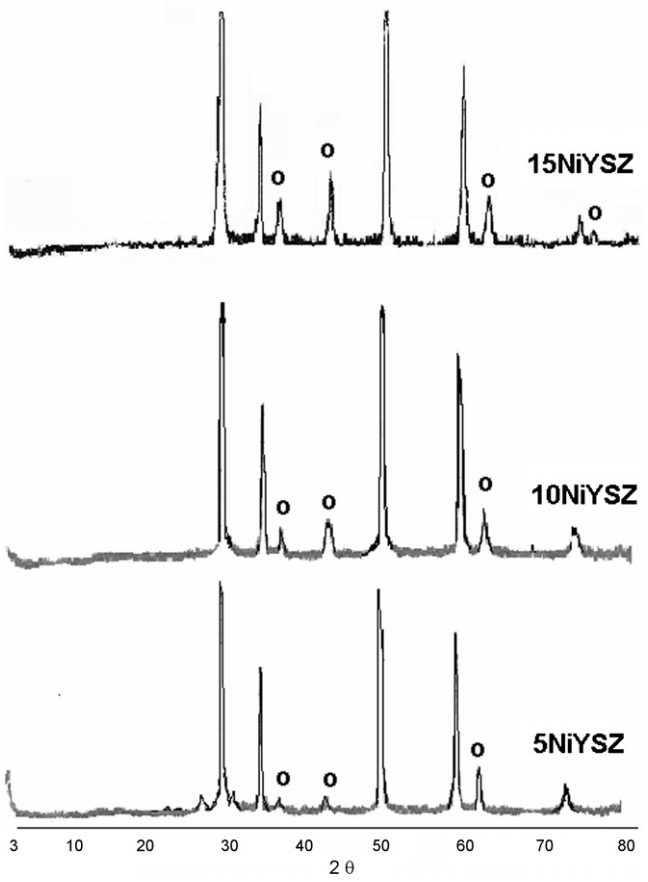

Fig. 7. X-ray diffraction patterns of the catalysts 5NiYSZ, 10NiYSZ and 15NiYSZ, NiO (◯).

Fig. 8 shows the TPR profiles of the catalysts supported on YSZ and the numerical values of the integrated peaks are listed in Table 4. Increasing the NiO load shifted the peaks to higher temperatures.

For the 5NiYSZ catalyst, reduction peaks are seen at 430 °C, 462 °C and 504 °C. The first peak (430 °C) is attributed in Section 3.1.1 to the reduction of NiO species in contact with oxygen

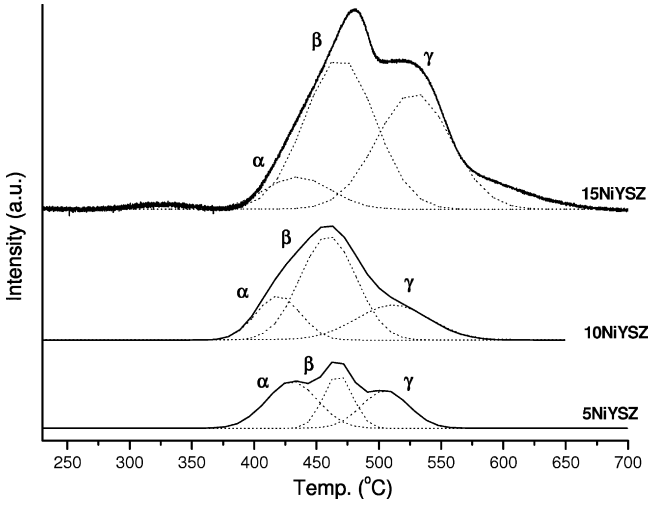

Fig. 8. TPR profiles of the catalysts 5NiYSZ, 10NiYSZ and 15NiYSZ.

Table 4
H_2 consumption of the nickel catalyst supported on YSZ

Catalyst	H_2 consumed $\times 10^{+5}$ (TPR peak temperature (°C))			Total H_2 consumed $\times 10^{+5}$
	α	β	γ	
5NiYSZ	1.7 (430)	1.1 (462)	1.3 (504)	4.1
10NiYSZ	1.6 (421)	4.4 (460)	1.9 (522)	7.9
15NiYSZ	1.5 (425)	6.8 (475)	5.5 (540)	13.8

vacancies in the YSZ. As already explained, the low reduction temperature may be due to the effect of the contact between the NiO species and the support in the neighborhood of its surface oxygen vacancies. Assuming that the number of surface oxygen vacancies is limited, the reduction of NiO species in contact with these vacancies should present a constant H_2 consumption (peak α in Table 4) and this behavior has been reported in many studies [25,26,28]. The reduction peaks at 462 °C and 504 °C were attributed to the reduction respectively of NiO species in the forms of crystallites and of NiO species in close contact with the support, but not with its surface oxygen vacancies. This may explain the growth of these two TPR peaks in the catalysts with 10 wt.% and 15 wt.% nickel loads. As can be seen in the XRD spectra (Fig. 7), the NiO crystallites are responsible for the XRD signals, whose intensities increase in parallel with the NiO load, while the TPR peaks around 460 °C, attributed to the reduction of NiO crystallites, are those that show the largest rise in H_2 consumption.

Figs. 9 and 10 show the composition profiles of the gaseous products of the steam reforming of ethanol over the 10NiYSZ and 15NiYSZ catalysts at 500 °C and 600 °C, where a stable behavior is observed in the composition of the gaseous products throughout 6 h of reaction. Table 5 shows the mean compositions of the products of these reactions.

In these catalytic tests, a total conversion of ethanol in the feed was observed. The presence of C_2H_4 was practically negligible as in the previous reactions. At 500 °C, the 10NiYSZ catalyst produced the higher proportion of CO_2 composition and this is due to the water–gas shift reaction (reaction (5)) being favored. This explanation is corroborated by a proportional decrease in the CO concentration and for the composition of liquid products in Table 6, where for the 10NiYSZ catalyst is seen to consume the most water. The proportion of CH_4 in the gaseous products was smallest on the 15NiYSZ catalyst and it can be assumed that the decomposition of ethanol (reaction (4)) is the principal path to the CH_4 produced. The low level of CH_4 on the 15NiYSZ catalyst may be due to the coke formation (reaction (6)) being favored by the high-nickel content in the crystallite form [32].

Comparing the catalytic test at 600 °C (Fig. 10) with the tests at 500 °C, it is observed that the water consumed increased on all the catalysts, and this increase was accompanied by a decrease in the CH_4 composition. This behavior indicates that, at 600 °C, the methane steam reforming (reaction (7)) is favored. The gaseous product compositions on the 5NiYSZ and 10NiYSZ catalysts showed the same profile, while the 15NiYSZ catalyst showed a low CO concentration and low water consumption, indicating that the steam reforming of methane occurs to a lesser extent than on the 5NiYSZ and 10NiYSZ catalysts. Therefore, the low con-

Table 5
Mean composition of gaseous products (%) of ethanol steam reforming

Temperature (°C)	Catalyst	Gaseous products (%)			
		H_2	CH_4	CO	CO_2
500	5NiYSZ	56	18	12	12
	10NiYSZ	60	17	8	18
	15NiYSZ	68	14	10	8
600	5NiYSZ	67	6	12	15
	10NiYSZ	66	6	12	16
	15NiYSZ	72	5	5	18

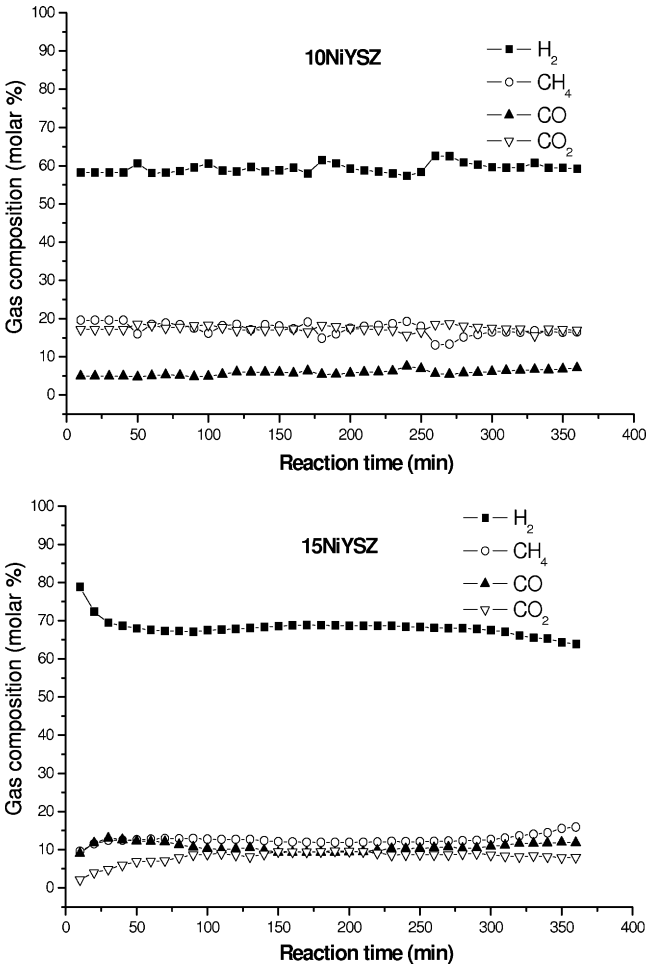

Fig. 9. Gas composition of the ethanol steam reforming products as a function of time of reaction. Reaction temperature 500 °C.

Table 6
Ethanol conversion and composition of liquid effluents for nickel catalyst supported on YSZ

Temperature (°C)	Catalyst	Volume of liquid effluents (mL)[a]		Water consumption (%)	Ethanol conversion (%)
		Acetaldehyde	Ethanol		
500	5NiYSZ	0.2	0.7	3	90.7
	10NiYSZ	–	–	25	98.7
	15NiYSZ	–	–	7	99.9
600	5NiYSZ	–	0.1	28	98.6
	10NiYSZ	0.1	1.0	40	98.8
	15NiYSZ	–	–	12	99.9

[a] Total volume collected during 6 h of reaction.

centrations of CH_4 and CO on the 15NiYSZ catalyst at 600 °C should be due to their consumption to produce coke (reactions (9) and (10)), for the same reasons presented at 500 °C for this catalyst.

Fig. 11 shows the hydrogen selectivity, where at 500 °C the best performance can be observed on the 10NiYSZ catalyst, while also shows the higher water consumption and CO_2 production, as mentioned previously. These results indicate that on the 10NiYSZ catalyst, the water–gas shift reaction can be strongly favored. The existence of nickel species interacting with the surface oxygen vacancies of the YSZ could be promoting the catalytic performance, activating the oxygenated species by the influence of these oxygen vacancies, which have an effective positive charge.

As the quantity of the surface oxygen vacancies is limited, the nickel species influenced by them are limited to and in this way, the catalytic results indicate that up to 10 wt.% of nickel load there is an increase of the nickel species in contact with the oxygen vacancies, which benefits the catalytic performance. When the nickel load increases to 15 wt.%, the hydrogen selectivity (at 500 °C) and the water consumption fall back, indicating that the extra nickel must be blocking the contact between the reacting molecules and the nickel species that enhanced the catalytic performance, namely the nickel species influenced by the oxygen vacancies. In the 15NiYSZ catalyst, the crystalline nickel species not influenced by the oxygen vacancies of the YSZ were

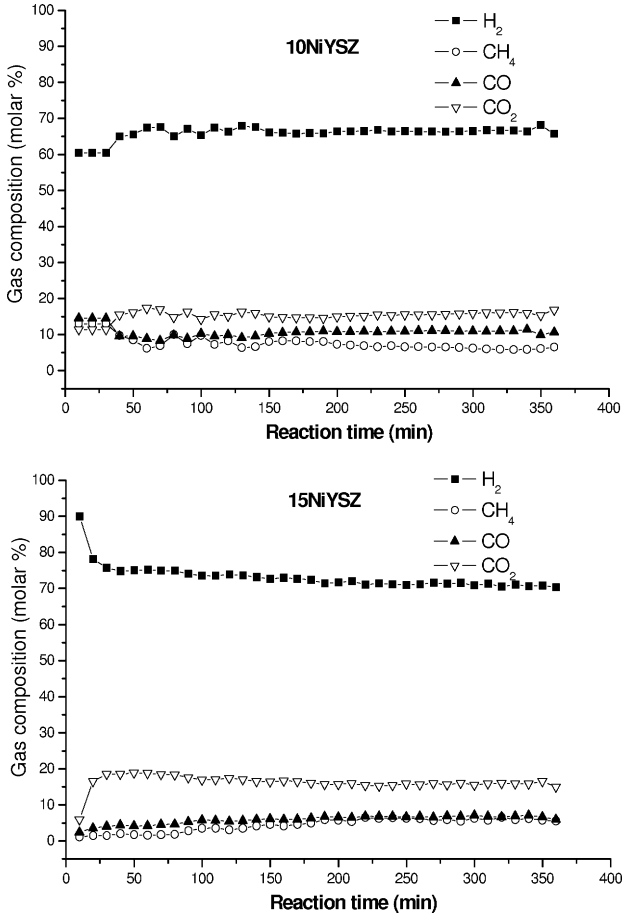

Fig. 10. Gas composition of the ethanol steam reforming products as a function of time of reaction. Reaction temperature 600 °C.

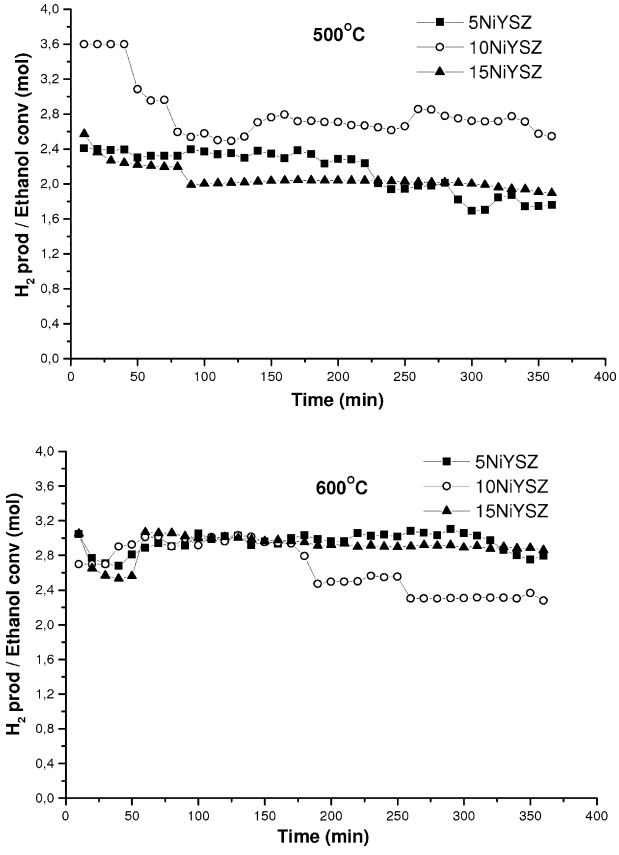

Fig. 11. Hydrogen selectivity for ethanol steam reforming at 500 °C and 600 °C on the nickel catalysts supported on YSZ.

observed in higher proportions (Fig. 8 and Table 4: peaks β and γ). At 600 °C, it is observed in Fig. 11 that the hydrogen selectivity improves, compared with the results at 500 °C, due mainly to the occurrence of methane steam reforming, indicated by the raised water consumption, mainly on the 10NiYSZ catalyst (Table 6).

For all reactions, the molar gas composition of products did not change during 6 h of reaction, showing no deactivation. Still, with respect to the stability of the reaction, it was performed one test for 10NiYSZ catalyst during 50 h at 600 °C (not shown), where it was observed that the reaction performance was stable with the molar gas composition of products constant during the reaction time.

Summarizing these results, all the catalysts showed activity for the steam reforming of ethanol, but a strong effect of the support on the product composition was observed; in other words, the modification of the ZrO_2 support with Y_2O_3 or CaO influenced the catalytic behavior of the nickel species supported there on. When the supports used were modified ZrO_2, the CO concentration decreased strongly, probably due to greater oxygen mobility, which arises from the increase in the number of oxygen vacancies in the modified ZrO_2, favoring an increase in CO_2 production. According to the results for the liquid products, these catalysts showed a high selectivity to the gaseous products, a small volume of acetaldehyde being the only liquid product observed. Other liquid products, such as acetic acid, ethyl ether and acetone were found in trace amounts.

4. Conclusion

In the catalyst series with 5 wt.% of nickel, it was observed that the modifications of the ZrO_2 support by incorporation of Y_2O_3 or CaO into the ZrO_2 lattice led to an increase in the CO_2 and H_2 content of the gaseous products. This behavior can be attributed to the presence of the oxygen vacancies in the support. The hydrogen selectivity was enhanced when the ZrO_2 was modified with Y_2O_3 (YSZ) but fell when the ZrO_2 was modified with CaO (CSZ), indicating that other interactions, in addition to those with the oxygen vacancies, were influencing the catalytic behavior of the nickel species.

In the catalyst series with nickel supported on YSZ (5NiYSZ, 10NiYSZ and 15NiYSZ), it was observed that the water–gas shift reaction, as much as methane steam reforming, was benefited by adding nickel up to 10 wt.% at both 500 °C and 600 °C, whereas at higher nickel load (15 wt.%), the performance of these reactions fell back, due to obstruction of the active nickel species by the nickel crystallites.

Acknowledgements

This work was funded by the CNPQ and FAPESP. We also are grateful to DEQ/UFSCar for the TPR and XRD measurements.

References

[1] V. Klouz, V. Fierro, P. Denton, H. Katz, J.P. Lisse, S. Bouvot-Mauduit, C. Mirodatos, J. Power Sources 105 (2002) 26.
[2] B.A. Peppley, J.C. Amphlett, L.M. Kearns, R.F. Mann, Appl. Catal. A 179 (1999) 21.
[3] B. Lindstrom, L.J. Pettersson, Int. J. Hydrogen Energy 26 (2001) 923.
[4] E.Y. Garcia, M.A. Laborde, Int. J. Hydrogen Energy 16 (1991) 307.
[5] Y. Wang, K. Murata, T. Hayakawa, S. Hamakawa, K. Suzuki, J. Chem. Technol. Biotechnol. 76 (2001) 265.
[6] K. Vasudeva, N. Mitra, P. Umansankar, S.C. Dhingra, Int. J. Hydrogen Energy 2 (1996) 13.
[7] D.K. Liguras, D.I. Kondarides, X.E. Verykios, Appl. Catal. B 43 (2003) 345.
[8] G. Maggio, S. Freni, S. Cavallaro, J. Power Sources 74 (2001) 17.
[9] M.S. Batista, R.K.S. Santos, E.M. Assaf, J.M. Assaf, E.A. Ticianelli, J. Power Sources 134 (2004) 27.
[10] S. Cavallaro, V. Chiodo, A. Vitaa, S. Freni, J. Power Sources 123 (2003) 10.
[11] S. Freni, J. Power Sources 94 (2001) 14.
[12] C. Diagne, H. Idriss, A. Kiennemann, Catal. Commun. 12 (2002) 565.
[13] D.K. Liguras, K. Goundani, X.E. Verykios, J. Power Sources 130 (2004) 30.
[14] J. Sun, X.P. Qiu, F. Wu, W.T. Zhu, Int. J. Hydrogen Energy 30 (2005) 437.
[15] F. Frusteri, S. Freni, V. Chiodo, L. Spadaro, G. Bonura, S. Cavallaro, J. Power Sources 132 (2004) 139.
[16] M.E.S. Hegarty, A.M. O'Connor, J.R.H. Ross, Catal. Today 42 (1998) 225.
[17] W.S. Dong, H.S. Roh, K.W. Jun, S.E. Park, T.S. Oh, Appl. Catal. A 226 (2002) 63.
[18] T. Takeguchi, S.N. Furukawa, M. Inoue, K. Eguchi, Appl. Catal. A 240 (2003) 223.
[19] P. Marcos, D. Gouvêa, Ceramica 50 (2004) 38.
[20] H. Teterytz, R. Klimkiewicz, M. Laniecki, Appl. Catal. A 249 (2003) 313.
[21] JCPDS, Diffraction Data Base (CD-ROM).
[22] H.S. Roh, W.S. Dong, K.W. Jung, S.E. Park, Chem. Lett. 30 (2001) 88.
[23] A.M. Diskin, R.H. Cunningham, R.M. Ormerod, Catal. Today 46 (1998) 147.
[24] R. Molina, G. Poncelet, J. Catal. 173 (1998) 257.
[25] Y. Chen, B. Liaw, C. Kao, J. Kuo, Appl. Catal. A 21 (2001) 23.
[26] W. Dow, Y. Wang, T. Huang, Appl. Catal. A 190 (2000) 25.
[27] J. Sun, X. Qiu, F. Wu, W. Zhu, W. Wang, S. Hao, Int. J Hydrogen Energy 29 (2004) 1075.
[28] W.P. Dow, T.J. Huang, J. Catal. 160 (1996) 171.
[29] J.M. Wei, B.Q. Xu, J.L. Li, Z.X. Cheng, Q.M. Zhu, Appl. Catal. A 196 (2000) L67.
[30] N.B. Jackson, J.G. Ekerdt, J. Catal. 126 (1990) 31.
[31] J.B. Wang, Y.L. Tai, W.P. Dow, T.J. Huang, Appl. Catal. A 218 (2001) 69.
[32] M. Bradford, M. Vannice, Appl. Catal. A 142 (1996) 73.